ARTICLE

Structure of Micelles of a Nonionic Block Copolymer Determined by SANS and SAXS

Sabine Manet,[†] Amélie Lecchi,[†] Marianne Impéror-Clerc,*,[†] Vladimir Zholobenko,[‡] Dominique Durand,[§] Cristiano L. P. Oliveira,[∥,○] Jan Skov Pedersen,[∥] Isabelle Grillo,[⊥] Florian Meneau,[#] and Cyrille Rochas[▽]

[†]Laboratoire de Physique de Solides, UMR 8502, Bât. 510, Université Paris-Sud, F-91405 Orsay, France

[‡]Chemistry Department, Keele University, Staffordshire, ST5 5BG, United Kingdom

[§]Institut de Biochimie et de Biophysique Moléculaire et Cellulaire, Bât. 430, Université Paris-Sud, F-91405 Orsay, France

[∥]Department of Chemistry and iNANO Interdisciplinary Nanoscience Center, Århus University, DK-8000 Århus, Denmark

[⊥]Institut Laue Langevin, BP 156, F-38042 Grenoble, France

[#]SWING, Synchrotron Soleil, BP 48, F-91192 Gif-sur-Yvette, France

[▽]D2AM, ESRF, 6 rue Jules Horowitz, F-38000 Grenoble, France

S *Supporting Information*

ABSTRACT: The micellar state of Pluronic P123, which is a poly-(ethylene oxide)-*b*-poly(propylene oxide)-*b*- poly(ethylene oxide) block polymer ($EO_{20}PO_{70}EO_{20}$), has been investigated using SANS, SAXS, and differential scanning calorimetry under the conditions utilized in the synthesis of ordered mesoporous materials, such as SBA-15. The absolute intensity measurements, both with SANS and SAXS, have provided a detailed quantitative description of the P123 micelles in the framework of a simple core—shell spherical model. The model developed has been used to establish the structure of the copolymer micelles, including their size, shape, aggregation number and detailed composition, as well as the structural changes induced by varying reaction conditions. The effects of temperature, pH, acidic source and the addition of swelling agents (toluene and TMB) are reported and discussed.
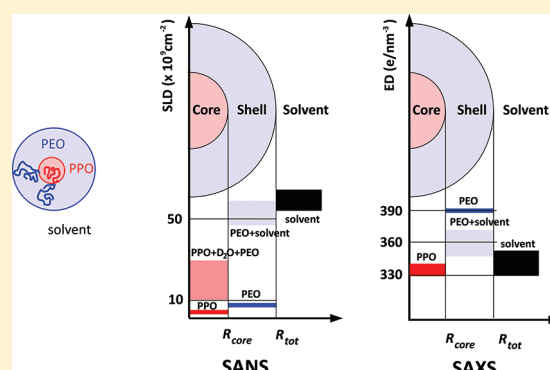
INTRODUCTION

Block copolymers of poly(ethylene oxide) and poly(propylene oxide) are commercial nonionic surfactants that are widely used in many research areas and industrial applications. One of these is the preparation of mesoporous materials, including the SBA family discovered in 1998.[1] During the synthesis of mesoporous materials, a silica precursor is added to an acidic copolymer solution and is hydrolyzed, forming cationic silicate species which condense around micellar aggregates in solution. This initial step is crucial in the formation mechanism of ordered mesostructured materials. The final mesoporous material is obtained by removing the copolymer via calcination or chemical treatment. In the case of SBA-15 materials made using Pluronic P123 triblock copolymer, the initial micelle size and shape are strongly modified during the synthesis process: the P123 spherical micelles in the reaction mixture grow and pack forming a 2-D hexagonal array within the structure of the final SBA-15 product.[2−5]

The first step in the investigation of the formation mechanism of these mesoporous materials[2−5] is to determine the structure of the micelles before the addition of the silica source. This structure may depend on a number of synthesis parameters: temperature, acidity, nature of the acid counterion, addition of a salt, an alcohol, or a

hydrophobic swelling agent. Although several recent publications have already reported the morphological changes of the micelles,[6−8] the effect of these different parameters is still not fully understood.

The aim of the present work is 2-fold: (i) to develop a model to ascertain how the preparation parameters can influence the size, shape, and composition of the micelles in the initial stages of SBA-15 synthesis and (ii) to use this model to establish the structure of the initial copolymer micelles and the hybrid organic—inorganic micellar species formed in the reaction mixture. This first paper is devoted to the structure of the micelles in absence of inorganic precursors. The second paper[9] focuses on the influence of the synthesis conditions on the formation mechanism of the hybrid organic—inorganic material after the addition of an inorganic precursor, and on the correlation between the final structure of the material and that of the micelles in the initial state.

In the present study, we focus on the micellar state of the Pluronic P123 poly(ethylene oxide)-*b*-poly(propylene oxide)-*b*-poly(ethylene oxide) (PEO-PPO-PEO) block polymer with the

Table 1. Composition in Molar Ratios of the P123 Solutions[a]

		D_2O									H_2O	
		HCl	HCl	HCl	TMB	TMB	TMB	toluene	toluene	toluene		HCl
sample	D_2O	2.5 M	1.6 M	0.2 M	C1	C2	C3	C1	C2	C3	H_2O	1.6 M
HCl		8.9	5.9	0.8	6	6	6	6	6	6		6
H_2O		30.8	20.5	2.7	20.7	20.7	20.7	20.7	20.7	20.7	197	197
D_2O	194.3	158.9	173.8	199.2	176	176	176	176	176	176		
$H_2O + D_2O$	194.3	189.8	194.3	201.8	196.7	196.7	196.7	196.7	196.7	196.7		197
P123	0.017	0.0176	0.017	0.0175	0.017	0.017	0.017	0.017	0.017	0.017	0.017	0.017
swelling agent (S.A.)					0.302	0.604	0.907	0.352	0.705	1.057		
R_{SA}					17.8	35.5	53.4	20.7	41.5	62.2		
pH	7	<0.1	<0.1	0.7	<0.1	<0.1	<0.1	<0.1	<0.1	<0.1	7	<0.1
c_{P123} (10^{-6} mol/mL)	4.72	4.74	4.56	4.65	4.45	4.41	4.36	4.46	4.41	4.37	4.65	4.49

[a] Two different swelling agents (SA) have been used, toluene (C_7H_8: TOL) and trimethylbenzene (C_9H_{12}: TMB), at three increasing concentrations (C1, C2, and C3) in 1.6 M aqueous solution of HCl and R_{SA} is the molar ratio of SA over P123. The composition of the solutions containing (HNO_3, HBr, H_2SO_4, and H_3PO_4) are given in Table SI.

composition $EO_{20}PO_{70}EO_{20}$ at a fixed concentration in water of 2.5 wt % (molar ratio water: P123 = 200:0.017). This copolymer is widely used to synthesize mesoporous materials, including SBA-15, and the concentration is within the optimum range for the formation of a well-organized material.

The structure of the micelles is investigated by small-angle scattering techniques, using both neutrons (SANS) and X-rays (SAXS), which are well-known powerful tools for the characterization of micelles in solution.[10−15] Contrary to the case of light scattering,[16] SANS and SAXS are sensitive to the internal structure of the scattering objects. The scattering curves are governed by the shape, size, and polydispersity of the scattering objects and their contrast with respect to the solvent. Using SAXS and SANS data, micelles can be described in a detailed way, including the properties of the hydrophobic core and the peripheral hydrophilic shell regions. The combination of SANS and SAXS data is helpful in this case, as it provides two different contrasts of the same micellar object. Although micelles of different Pluronic copolymers in water have been widely studied using such scattering techniques,[10−15,17] in this work we aim to provide a quite complete data set for Pluronic P123 investigated in situ during the synthesis of SBA-15 materials.

The modeling of the scattering by micelles of nonionic surfactants has been reported in the literature.[18] The theoretical basis of the scattering data analysis is well established and is recalled in details in this communication, including in the Supporting Information (SI) section. We choose to simulate the micelles using a simple core−shell two density levels model, mainly because this type of core−shell model will be applied throughout the modeling of the kinetic experiments,[9] allowing one to locate as a function of reaction time the silica species interactions with the micelles. More refined models for nonionic micelles have been already introduced in the literature, especially to better describe the density distribution inside the hydrophilic part, using for example individual grafted PEO chains on an homogeneous hydrophobic core,[19] but this later model is more suited to the case of nonionic copolymer with long hydrophilic segments (typically more than one hundred EO units).[20] As the P123 copolymer has hydrophilic chains with only 20 EO groups, the simpler core−shell model is still adequate, and has the advantage of introducing a relatively low number of seven

independent parameters in the fitting procedure. We take advantage of the absolute intensity measurements, performed both with SANS and SAXS, to derive a quantitative description of the micelles in terms of the aggregation number N_{agg} and of the absolute values of the density levels, ρ_{core} and ρ_{shell}. This description is based not only on the fit parameter values of the core−shell model, but on some other physicochemical data of the system: The known concentration of P123, c_{P123}, and the apparent partial specific densities (g/cm^3), estimated from literature values, of the different components of the solutions: The solvent, the PPO and PEO blocks and the swelling agents.

Our work demonstrates that this model is sufficient to establish the influence of the synthesis parameters on the micelle structure. Following the description of the experimental methods (DSC, SANS, and SAXS) and the theoretical basis of the scattering data analysis, the role of reaction temperature (SANS and SAXS), the acid concentration (DSC, SANS, and SAXS) and the addition of a swelling agent (SANS) are investigated and discussed.

■ EXPERIMENTAL METHODS

Sample Preparation. Pluronic P123 (Aldrich) was used as received to make aqueous solutions containing a range of organic and inorganic constituents. Deuterated water (D_2O) instead of H_2O was used as a solvent for the SANS measurements. The molar ratio water: P123 was kept close to 200:0.017 for all the samples corresponding to a molar concentration close to 4.5×10^{-6} mol/cm^3. Four series of samples were prepared (Table 1 and Table SI): (i) P123 solutions with different concentration of HCl for variable temperature SANS and DSC experiments, (ii) P123 solutions containing two different swelling agents (SA), toluene (C_7H_8: TOL) and trimethylbenzene (C_9H_{12}: TMB) at three increasing concentrations (C1, C2, and C3) prepared in 1.6 M aqueous solution of HCl for SANS, (iii) P123 solutions prepared in H_2O and D_2O for SAXS, and (iv) P123 solutions with different acids (HNO_3, HBr, HCl, H_2SO_4, and H_3PO_4) at the same proton concentration ([H^+] = 1.6 M, except in the case of the weak acid H_3PO_4 for which only the counterion concentration was kept constant) investigated at 40 °C with SAXS (Table SI).

For the samples prepared for SANS in D_2O in acidic conditions (i) and (ii), concentrated acidic solutions in H_2O were used as acidic source, and then the samples contained a mixture of D_2O and H_2O (Table 1).

DSC. Differential scanning calorimetry (DSC) measurements were carried out with a Micro DSC III apparatus from SETAR-AM which allows high sensitivity with dilute solutions. Samples of about 0.6 g were investigated at heating/cooling rates of 0.1, 0.4, and 0.6 °C/min to ensure the reversibility of the transition at temperatures ranging from 10 to 80 °C. The samples were placed in hastelloy cells and D_2O was used as reference.

SANS (Small Angle Neutron Scattering). SANS experiments were performed on the D22 spectrometer of the Institute Laue-Langevin, Grenoble, France. The neutron wavelength was 0.6 nm, with a wavelength spread (fwhm) of $\Delta\lambda$ = 10%, and the beam size was 0.7 cm^2 at the sample position. The data were recorded at two different sample–detector distances of 5 m (beam intensity = 5.6×10^6 neutrons/s for a range of scattering vector moduli q from 1×10^{-2} to 2×10^{-1} $Å^{-1}$) and 17 m (beam intensity = 1.5×10^6 neutrons/s for a q range from 3×10^{-3} to 6×10^{-2} $Å^{-1}$). Note that the scattering vector modulus $q = 4\pi \sin \theta/\lambda$, where 2θ is the scattering angle and λ is the wavelength. Absolute scale intensities (cm^{-1}) were obtained by calibration using the incoherent scattering signal from a 1-mm thick water sample.

SAXS (Small Angle X-ray Scattering). SAXS measurements were carried out at the D2AM ESRF beamline (energy 11 keV) and at the SWING SOLEIL beamline (energy 12 keV). At D2AM, the sample–detector distance was 1.623 m, and the q range was 1.0×10^{-3}–1.57×10^{-1} $Å^{-1}$. At SWING, the sample–detector distance was 3.28 m, and the q range was 3.3×10^{-4}–1.57×10^{-1} $Å^{-1}$. In both cases, the q range calibration was made using a silver behenate standard sample (d_{ref} = 58.38 Å).

For the absolute intensity calibration, scattering patterns of the empty capillary and the capillary filled with deionized water were always recorded before the introduction of the Pluronic solutions. The value of the constant intensity contribution of water is equal to 0.016 cm^{-1} on absolute scale.[21] In addition, both the signal of the capillary filled with the solvent solution and with the micellar solution were recorded for subtraction purposes. During these measurements, the capillaries were kept fixed inside the beam using a capillary holder, so that all patterns were recorded at the same position.

For SAXS, the scattering length density is the product of the classical radius of the electron r_e = 2.81794×10^{-15} m and the electron density (number of electrons per unit volume). In the tables, we give the electron density (ED) values in e/nm^3 rather than the scattering length density (SLD), but the coefficient r_e is taken into account for the absolute scaling (in cm^{-1}) in the intensity expression.

Values of the SLD and ED. The values of the coherent neutron scattering lengths were taken from the NIST database.[22] For the different solvents (H_2O, D_2O, and acidic solutions) (Table 2), the electron densities and scattering length densities were determined from the density values in function of temperature using literature data.[23] In the case of the acidic solutions, the SLD values were calculated, assuming the same specific volumes as in pure H_2O, and taking into account the relative proportions of H_2O and D_2O in each sample (Table 1). For PPO and PEO, the SLD and ED values were derived from the experimental values of their apparent specific volume in the micellar state (Table 2).[24]

Table 2. Values of the Density, Molecular Volumes V, Coherent Neutron Scattering Length Density (SLD), and Electron Density (ED) versus Temperature

T, °C	PO density, g/cm^3	PO V, $Å^3$	PO SLD, cm^{-2}	PO ED, e/nm^3	EO density, g/cm^3	EO V, $Å^3$	EO SLD, cm^{-2}	EO ED, e/nm^3	H_2O density, g/cm^3	H_2O SLD, cm^{-2}	D_2O density, g/cm^3	D_2O SLD, cm^{-2}	H_2O/D_2O V, $Å^3$	H_2O/D_2O ED, e/nm^3	HCl 1.6 M density, g/cm^3	HCl 1.6 M SLD, cm^{-2}	HCl 1.6 M ED, e/nm^3
20	1.01	96	3.43×10^9	334	1.20	61	6.80×10^9	394	0.998	-5.59×10^9	1.110	6.39×10^{10}	29.97	334	1.027	5.54×10^{10}	341
40	1.00	96	3.42×10^9	333	1.18	62	6.67×10^9	387	0.992	-5.56×10^9	1.104	6.36×10^{10}	30.15	332	1.020	5.50×10^{10}	339
60	0.99	97	3.41×10^9	330	1.16	63	6.54×10^9	379	0.983	-5.50×10^9	1.093	6.29×10^{10}	30.43	329	1.011	5.46×10^{10}	336

11320

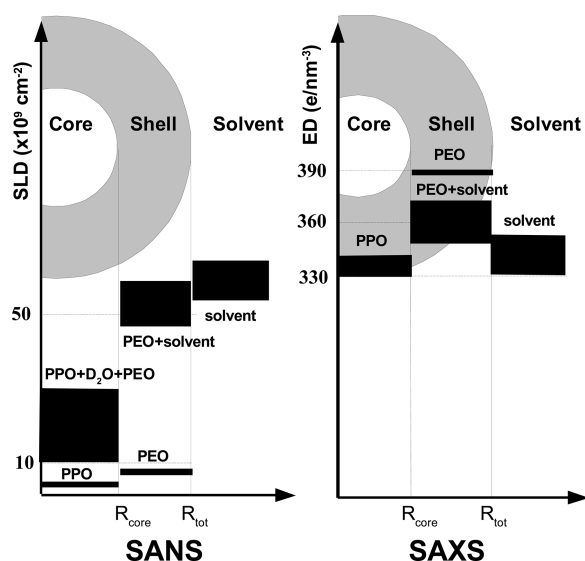dx.doi.org/10.1021/jp200212g |*J. Phys. Chem. B* 2011, 115, 11318–11329

Figure 1. Core—shell density model for SANS and SAXS.

For the swelling agents, the values of the scattering length densities are for toluene, per-deuterated toluene and trimethylbenzene $\rho_{TOL} = 9.3 \times 10^9 \text{ cm}^{-2}$, $\rho_{dTOL} = 56.15 \times 10^9 \text{ cm}^{-2}$, and $\rho_{TMB} = 6.7 \times 10^9 \text{ cm}^{-2}$ and have been derived from the bulk densities at room temperature. The scattering length density of the solvent is the same for all the samples containing swelling agents: $\rho_0 = 5.54 \times 10^{10} \text{ cm}^{-2}$ at 20 °C and $\rho_0 = 5.50 \times 10^{10} \text{ cm}^{-2}$ at 40 °C.

■ THEORETICAL MODEL

As already mentioned, the micelles are described by a core—shell model where the core and the shell have uniform densities (Figure 1). The contrast of the experimental patterns can be rather different for the same objects for SANS and SAXS. For SANS, the contrast depends on the values of the nuclear scattering length densities (SLD, in cm^{-2}), and for SAXS, it depends on the values of the electron densities (ED, in e/nm^3; Table 2).

The scattered intensity $I(q)$ as a function of the scattering vector q can be taken as a product of a form factor term and a structure factor term

$$I(q) = AP(q, R_{core}, R_{tot}, \alpha, \sigma)S(q, R_{HS}, \phi_{PY}) \qquad (1)$$

with

$$P(q, R_{core}, R_{tot}, \alpha, \sigma) = \langle F^2(q, R_{core}, R_{tot}, \alpha)\rangle_{poly}$$

$$= \int f(R, R_{core}, \sigma)[F(q, R, RR_{tot}/R_{core}, \alpha)]^2 \, dR \qquad (2)$$

where $F(q, R_{core}, R_{tot}, \alpha)$ is the amplitude of the form factor for the core—shell model of spherical objects

$$F(q, R_{core}, R_{tot}, \alpha) = (1 - \alpha)V(R_{core})F_S(q, R_{core})$$
$$+ \alpha V(R_{tot})F_S(q, R_{tot}) \qquad (3)$$

with $F_s(q, R) = 3(\sin(qR) - qR\cos(qR)/(qR)^3$ and $V(R) = (4\pi/3)R^3$.

$f(R, R_{core}, \sigma) = f_{SZ}(R, R_{core}, 1/\sigma^2 - 1)$ is the polydispersity distribution, taken as a Schulz—Zimm distribution, of the micelles radii and $S(q, R_{HS}, \phi_{HS})$ is the structure factor contribution, taken as the Percus—Yevick (PY) expression for hard-spheres.

For SANS there is a significant instrumental smearing of the scattering intensity and the expression used for the scattered intensity has to be described by the convolution product of $I(q)$ with an experimental resolution function.[25] Further details are given in the S. I.

In the current model, the core and the shell are assumed to have uniform scattering length densities, ρ_{core} and ρ_{shell}. The value of the solvent scattering length density ρ_0 is a known quantity for each temperature and composition and is given in Table 2. A relatively low number of seven independent parameters (R_{core}, R_{tot}, α, σ, A, R_{HS}, ϕ_{PY}) are included in the fitting procedure: The two sizes, R_{core} and R_{tot}, the density levels ratio, $\alpha = (\rho_{shell} - \rho_0)/(\rho_{core} - \rho_0)$, the polydispersity factor σ, the two PY-structure factor parameters (R_{HS}, ϕ_{HS}) and the overall scaling factor, A, which below is related to the aggregation number and the core contrast.

The variations of the intensity are essentially governed by the polydisperse form factor contribution which depends on the four parameters (R_{core}, R_{tot}, α, σ). The structure factor term $S(q, R_{HS}, \phi_{PY})$ is mainly equal to 1, except in the low-q region with q less than 0.02 Å^{-1}. In the case of SANS, the values found for the fit parameter α (see Figure 1 and Table 3) are close to 0.1. It means that the contribution of the shell region is much less compared to the one of the core region. However, it was checked that a pure core model (imposing $\alpha = 0$) gives poor fits, with significantly larger chi-squared χ^2 values. This justifies the use of a complete core—shell model for SANS.

After the optimization of the fit parameter values, we take advantage of the absolute intensity measurements, performed both with SANS and SAXS, to derive a quantitative description of the micelles, in terms of the aggregation number N_{agg} and of the absolute values of the density levels, ρ_{core} and ρ_{shell}. This allows us to provide the two values of ρ_{core} and ρ_{shell}, and not only the relative contrast with respect to the solvent using the parameter $\alpha = (\rho_{shell} - \rho_0)/(\rho_{core} - \rho_0)$. More precisely, absolute scale provides a value of the scaling factor A in cm^{-7} and not in arbitrary scale. The expression of the scaling factor is $A = n(\rho_{core} - \rho_0)^2$ where n is the micelle number density. It is then possible to derive values of N_{agg}, ρ_{core} and ρ_{shell}, based on some of the fit parameters values (R_{core}, R_{tot}, $\alpha = (\rho_{shell} - \rho_0)/(\rho_{core} - \rho_0)$, $A = n(\rho_{core} - \rho_0)^2 = (c_{P123}N_A/N_{Agg})(\rho_{core} - \rho_0)^2$) but it is also necessary to include some simple additional assumptions about the structure of the micelles that are detailed below. These additional assumptions are needed in order to separate in the scale factor A the contributions of the micelle number density n and the contrast term $(\rho_{core} - \rho_0)^2$ that appear as a product.

First, the concentration in P123, c_{P123}, ($4-5 \times 10^{-6} \text{ mol/cm}^3$) is fixed. It is related to the micelle number density $n = c_{P123}N_A/N_{Agg}$ where N_A is the Avogadro's number and N_{Agg} is the aggregation number. The accurate value of c_{P123} for the different samples is calculated from the molar composition and is reported in Table 1. One can neglect the fact that a small fraction of the P123 molecules is in the monomer form, as the value of the CMC (10^{-8} to $10^{-10} \text{ mol/cm}^3$)[26] is much smaller than c_{P123} in the temperature range we investigated. Second, the densities (g/cm³) values in function of temperature of the different components (solvent, PPO, PEO blocks and the swelling agents) of the solutions are introduced (Table 2). Obviously, the precision on the obtained values of N_{agg}, ρ_{core}, and ρ_{shell} depends strongly on the accuracy of the concentration c_{P123}, the density values, especially in the case of SAXS, where the contrasts are weak. Then, the following assumptions about the repartition of the

Table 3. SANS Results: Effect of the Temperature and HCl Concentration on the Structure and Composition of P123 Micelles[a]

SANS	D$_2$O		HCl 0.2 M	HCl 1.6 M			HCl 2.5 M
parameters	20 °C	40 °C	40 °C	20 °C	40 °C	60 °C	40 °C
A (10^{37} cm^{-7})	5.08 ± 0.02	5.03 ± 0.02	5.04 ± 0.02	3.91 ± 0.03	4.05 ± 0.02	2.89 ± 0.01	3.79 ± 0.02
$A\,P(0)$ (cm^{-1})	85.5 ± 0.4	118.5 ± 0.3	118.3 ± 0.4	42.6 ± 0.3	83.6 ± 0.3	150.5 ± 0.4	65.2 ± 0.3
R_{core} (nm)	6.1 ± 0.05	6.5 ± 0.05	6.5 ± 0.05	5.7 ± 0.05	6.4 ± 0.05	7.2 ± 0.05	6.1 ± 0.05
R_{tot} (nm)	9.1 ± 0.05	9.3 ± 0.05	9.3 ± 0.05	8.8 ± 0.1	9.1 ± 0.05	9.8 ± 0.05	9.0 ± 0.05
α	0.097 ± 0.002	0.119 ± 0.002	0.113 ± 0.002	0.058 ± 0.003	0.118 ± 0.002	0.162 ± 0.003	0.108 ± 0.003
σ (%)	12.6 ± 0.1	10.8 ± 0.1	10.8 ± 0.1	13.4 ± 0.2	10.7 ± 0.1	15.1 ± 0.1	11.3 ± 0.1
ϕ_{HS}	0.066 ± 0.001	0.063 ± 0.001	0.063 ± 0.001	0.060 ± 0.002	0.065 ± 0.001	0.0095 ± 0.001	0.069 ± 0.001
R_{HS} (nm)	9.5 ± 0.1	9.6 ± 0.1	9.6 ± 0.1	8.8 ± 0.3	9. 6 ±0.1	12.7 ± 0.5	9.3 ± 0.1
χ^2	2.7	1.6	2.1	2.1	1.8	2.0	1.9
c (10^{-6} mol/mL)	4.72 ± 0.1		4.65 ± 0.1		4.56 ± 0.1		4.74 ± 0.1
ρ_0 (10^{10} cm^{-2})	6.39	6.36	6.25	5.54	5.50	5.46	5.07
N_{agg}	81 ± 4	117 ± 6	122 ± 6	54 ± 3	113 ± 6	180 ± 9	101 ± 5
n (10^{16} cm^{-3})	3.5	2.4	2.3	4.8	2.3	1.4	2.6
ϕ_{tot}	0.11	0.08	0.08	0.14	0.07	0.06	0.08
ρ_{core} (10^{10} cm^{-2})	2.57	1.81	1.57	2.78	1.41	1.10	1.41
ρ_{shell} (10^{10} cm^{-2})	6.02	5.82	5.72	5.38	5.02	4.75	4.67
x (%)	94	90	91	97	90	85	91
pEO shell (%)	72	73	70	52	75	77	75
y_{POcore} (%)	57	69	72	46	73	79	72
y_{EOcore} (%)	6	7	8	8	7	7	7
$y_{water\ core}$ (%)	37	24	20	46	20	14	21
R_{PO} (nm)	5.1	5.7	5.8	4.4	5.7	6.7	5.5

[a] Notations are given in the theoretical model section.

P123 copolymer in the micelles are made. We assume that all is included in the core+shell region with the ratio PPO:PEO = 70:40 imposed by the copolymer sequence (EO$_{20}$PO$_{70}$EO$_{20}$). Then, it is assumed that the shell contains only EO groups and solvent as the core is composed of all of the PO groups, of water, and of the remaining EO groups. In the case of SANS, the hypothesis of a core containing only PO groups appears to be incompatible with the fit results, mainly because it imposes a too small value of ρ_{core}, that is not consistent with the values of A and c_{P123} and a satisfactory model of the PPO/PEO repartition within the micelles. On the contrary, in the case of SAXS, the hypothesis of a core corresponding to the PPO groups provides a good description. As detailed after in the paper, this is related to the difference of contrasts between SAXS and SANS (figure 1). Especially, as the ED of PO and water are very close to each other, it is not possible to quantify the core hydration level using SAXS.

Then, enough independent relations between all of the different parameters are provided within this model and all of the parameters values can be determined. These relations are given in the SI. When a swelling agent (SA) is present, two closely related hypotheses (see the SI for details) are compared to check if all the swelling agent molecules are incorporated inside the micelles or not: One assumes that the SA is completely included in the core region, or that no EO groups are present inside the core. Finally, the fit results are interpreted using the following quantities: N_{agg}, ρ_{core}, ρ_{shell}, x, the volume fraction of solvent inside the shell, p_{EO}, the proportion of the EO groups of a P123 molecule inside the shell, and the different volume fractions in the core: y_{PO}, y_{EO} (and y_{SA} for a swelling agent). The total micellar volume fraction defined as $\phi_{tot} = n\,V(R_{tot})$ is also given in the Tables. In addition, for SANS, the equivalent radius R_{PO}

of the sphere containing only the PO groups ($V(R_{PO})$ = $N_{agg}70v_{PO}$) is given (Table 3) to allow comparison with the core radius derived from the SAXS measurements (Table 4). R_{SA} is the molar ratio of swelling agent over P123 (Tables 1 and 5).

■ RESULTS

Effect of Temperature (SANS). The structure of the P123 micelles has been investigated at three different temperatures: 20, 40, and 60 °C covering their range of stability[16] (Figure 2A and Table 3). On increasing temperature, the core radius R_{core} of the micelles is increasing, and, accordingly, the aggregation number N_{Agg} is increasing. The polydispersity of the size of the micelles is between 10 and 15%. Interestingly, it shows a minimum at 40 °C for HCl 1.6 M: σ = 13.4% (20 °C), 10.7% (40 °C), and 15.1% (58 °C). This effect may be related to the vicinity of the CMT at 20 °C and to the stability limit at 60 °C, and 40 °C appears to be an optimal temperature for the formation of P123 micelles. Complementary SAXS results (Table 4) performed at 40 °C give a polydispersity of σ = 10%, in good agreement with the SANS value.

The composition of the core and shell derived from the model for the SANS results (Table 3) allows us to quantify a progressive dehydration of the micelles on increasing temperature. The shell is always highly hydrated, with a solvent volume fraction x close to 90%. This hydration level of the shell decreases slightly upon temperature. The proportion p_{EO} of the EO groups located inside the shell do not evolve much with temperature, and its value is about 75%. The remaining EO groups correspond to only a small volume fraction of the core y_{EO}, close to 7%. Then, in this model, the core is mainly composed by the PO groups and by

Table 4. SAXS Results for P123 Solutions (2.5% w/w) in 1.6 M HCl at 40°C with Different Acids (HNO$_3$, HBr, HCl, H$_2$SO$_4$, and H$_3$PO$_4$) Recorded at the SOLEIL Synchrotron (Figure 4)^a

parameters	HNO$_3$	HBr	HCl	HCl (D2AM)	H$_2$SO$_4$	H$_3$PO$_4$
A (10^{35} cm^{-7})	2.02 ± 0.03	5.07 ± 0.5	0.91 ± 0.02	1.17 ± 0.01	4.9 ± 0.2	7.3 ± 0.2
$A\,P(0)$ (cm^{-1})	0.16 ± 0.002	0.0062 ± 0.0006	0.193 ± 0.003	0.152 ± 0.002	0.0068 ± 0.0002	0.067 ± 0.01
R_{core} (nm)	4.5 ± 0.05	5.3 ± 0.05	5.4 ± 0.05	5.6 ± 0.05	5.6 ± 0.05	5.8 ± 0.05
R_{tot} (nm)	6.5 ± 0.05	7.4 ± 0.05	8.4 ± 0.05	8.0 ± 0.05	9.1 ± 0.05	9.6 ± 0.05
α	−1.45 ± 0.03	−0.68 ± 0.02	−1.08 ± 0.02	−1.27 ± 0.03	−0.26 ± 0.01	−0.18 ± 0.01
σ (%)	18.2 ± 0.2	14.0 ± 0.2	10 ± 0.2	9.9 ± 0.2	9.4 ± 0.2	8.2 ± 0.3
ϕ_{HS}	0.064			0.052		
R_{HS} (nm)	7.6 ± 0.3			8.5 ± 0.5		
χ^2	5.8	15	6.7	42	8.7	17
c (10^{-6} mol/mL)	4.38 ± 0.1	4.45 ± 0.1	4.48 ± 0.1	4.48 ± 0.1	4.45 ± 0.1	4.28 ± 0.1
N_{agg}	57 ± 3	94 ± 5	97 ± 5	109 ± 6	109 ± 6	122 ± 6
n (10^{16} cm^{-3})	4.7	2.9	2.8	2.5	2.5	2.1
ϕ_{tot}	0.05	0.05	0.07	0.05	0.08	0.08
$|\rho_{core} - \rho_0|^*$ (e/nm^{-3})	7 ± 2	15 ± 3	6 ± 1	8 ± 2	16 ± 3	21 ± 4
ρ_0 (e/nm^{-3})	348 ± 2	354 ± 2	339 ± 2	339 ± 2	346 ± 2	345 ± 2
ρ_{core} (e/nm^{-3})	333 ± 3	333 ± 3	333 ± 3	333 ± 3	333 ± 3	333 ± 3
$(\rho_{core} - \rho_0)$ (e/nm^{-3})	15 ± 5	21 ± 5	6 ± 5	6 ± 5	13 ± 5	12 ± 5
x (%)	82	78	87	81	89	90
ρ_{shell} (e/nm^{-3})	370 ± 5	368 ± 4	345 ± 4	347 ± 5	349 ± 3	347 ± 3
$\rho_{shell\ sol}$ (e/nm^{-3})	366 ± 5	363 ± 4	339 ± 4	337 ± 5	345 ± 3	343 ± 3

^{a} For HCl, the results obtained at the ESRF (D2AM) are given for comparison (see Figure 2B). Notations are given in the main text and the SI section.

water. The volume fraction of water in the core y_{water} is quite high at 20 °C (40%) and decreases to a value of 20% or less at higher temperatures. These values are in good agreement with previous results obtained for a similar triblock copolymer (EO$_{25}$PO$_{40}$-EO$_{25}$) by modeling SANS data.[19] As expected, the micelles are much more hydrated at 20 °C, close to their micellization temperature[14] (see below the DSC results) than at higher temperatures. On increasing temperature, the driving phenomenon is the progressive dehydration of the PO groups.

The temperature of 60 °C is very close to the stability limit of the spherical micelles.[16] This is in agreement with the complementary SAXS measurements (Figure SI) showing considerable changes in the scattering curves at 60 °C, which can no longer be described using a model based on the spherical shape of the micelles, and possibly, cylindrical micelles are formed.[7]

Effect of HCl Acid Concentration (DSC and SANS). DSC measurements for an acidified solution of Pluronic in 2.5 M HCl and for an equivalent solution without the acid in pure D$_2$O are compared in Figure 3. Values for the transition temperature T_{onset}, which defines the CMT (critical micellization temperature)[27] and enthalpy changes are given. DSC traces for both samples show an endothermic transition peak corresponding to the formation of micelles around 20 °C. The addition of HCl induces the shift of micellization toward higher temperatures with the CMT increasing by 6 °C. The micellization enthalpy decreases with the addition of HCl.

The effect of the HCl concentration (0.2 M, 1.6 and 2.5 M) on the structure of the micelles has been investigated by SANS at 40 °C (Table 3). The dimensions of the micelles do not evolve much on increasing HCl concentration, with a value of R_{tot} always close to 9.1 nm and a value of R_{core} slightly decreasing (from 6.5 to 6.1 nm). No significant evolution of the hydration levels is observed on the HCl concentration, with values always close to those in pure water at the same temperature. The main

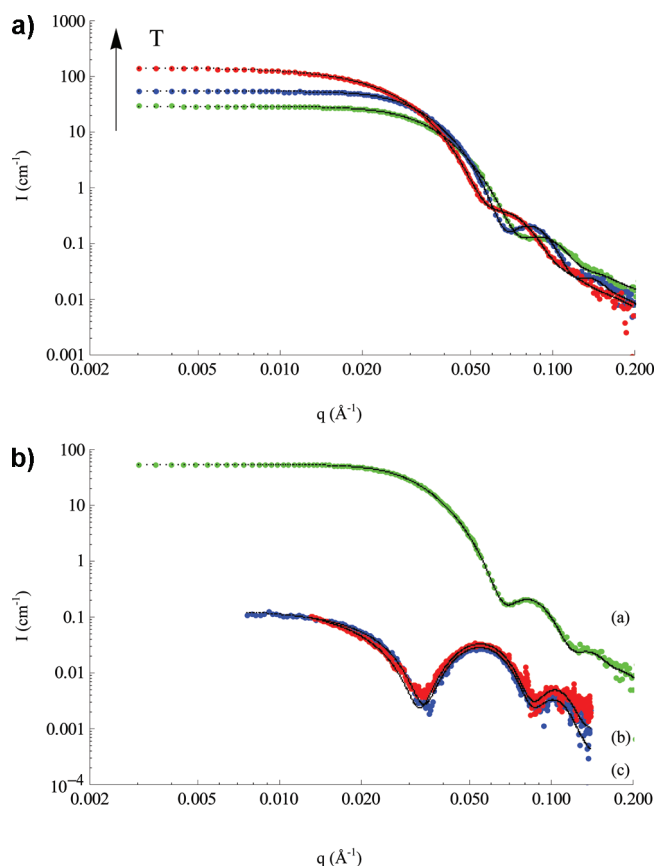evolution is a decrease of the aggregation number N_{Agg} from 117 without HCl to 101 in 2.5 M HCl.

Figure 2B presents a comparison of the absolute intensity profiles in cm^{-1}, obtained from SANS and SAXS measurements, for the same sample (P123 in HCl 1.6 M at 40 °C) showing both the experimental data and the curves fitted using the core−shell model. This comparison demonstrates that the SANS contrast gives rise to higher scattering intensities with good statistics, whereas the SAXS data show a much lower signal-to-noise ratio. This sample has been characterized by SAXS at two different synchrotron beamlines, D2AM (ESRF) and SWING (SOLEIL), and the results of absolute scaling are very close, thus validating the calibration method for SAXS using water (Table 4). The number density of scattering objects obtained for SAXS ($n = 2.5 \times 10^{16}$ cm^{-3} (D2AM) and 2.8×10^{16} cm^{-3} (SOLEIL)) is in good agreement with the one obtained from the SANS result ($n = 2.3 \times 10^{16}$ cm^{-3}). A reasonable agreement is also obtained for the aggregation numbers between SAXS ($N_{agg} = 109 \pm 6$ (D2AM) and 97 ± 5 (SOLEIL)) and SANS ($N_{agg} = 113 \pm 6$). The SAXS data are modeled making the assumption that the core is occupied by the PO groups and, in this case, the value of $R_{core} = 5.5$ nm deduced from SAXS compares well with the equivalent radius $R_{PO} = 5.7$ nm deduced from the SANS model. This result shows that the two types of scattering techniques converge giving an adequate description of the micellar solution. Interestingly, the values of R_{core} and R_{tot} are always significantly smaller for the SAXS data analysis as compared to that from SANS; this is considered in more details in the discussion section.

Overall, a simple core−shell model, developed in this work, with the core and the shell having uniform densities, provides a detailed description of the Pluronic micelles in P123: H$_2$O: HCl systems, including their shape, size, polydispersity and composition of the core and shell regions, as well as the micelle concentration and aggregation numbers. Our results help to

Table 5. SANS Results: Effect of the Addition of a Swelling Agent (SA)[a]

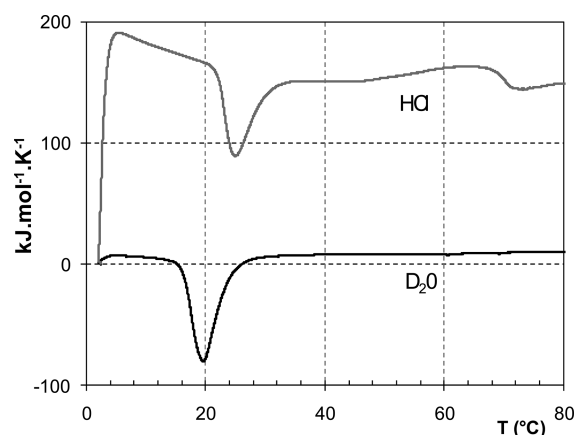| parameters	20 °C			40 °C			20 °C			40 °C		
	TMB C1	TMB C2	TMB C3	TMB C1	TMB C2	TMB C3	toluene C1	toluene C2	toluene C3	toluene C1	toluene C2	toluene C3
A (10^{37} cm^{-7})	1.93 ± 0.02	1.79 ± 0.02	1.72 ± 0.02	1.73 ± 0.02	1.44 ± 0.02	1.39 ± 0.02	1.91 ± 0.02	2.04 ± 0.02	1.57 ± 0.02	2.38 ± 0.02	2.06 ± 0.02	1.61 ± 0.02
$A\,P(0)$ (cm^{-1})	309 ± 2	737 ± 6	730 ± 7	304 ± 2	636 ± 4	779 ± 6	297 ± 2	302 ± 2	566 ± 3	213 ± 2	280 ± 2	532 ± 3
R_{core} (nm)	9.1 ± 0.05	10.5 ± 0.05	10.5 ± 0.05	9.3 ± 0.05	10.8 ± 0.05	11.1 ± 0.05	9.1 ± 0.05	9.0 ± 0.05	10.6 ± 0.05	8.3 ± 0.05	8.9 ± 0.05	10.4 ± 0.05
R_{tot} (nm)	12.2 ± 0.05	13.7 ± 0.05	13.3 ± 0.1	12.2 ± 0.05	13.6 ± 0.06	13.8 ± 0.06	12.0 ± 0.05	12.1 ± 0.05	13.2 ± 0.05	10.9 ± 0.07	11.5 ± 0.07	13.2 ± 0.07
α	0.125 ± 0.005	0.14 ± 0.005	0.16 ± 0.010	0.126 ± 0.005	0.13 ± 0.005	0.14 ± 0.005	0.127 ± 0.005	0.101 ± 0.005	0.109 ± 0.005	0.131 ± 0.010	0.130 ± 0.010	0.111 ± 0.005
σ (%)	9.9 ± 0.1	13.0 ± 0.1	13.9 ± 0.2	9.2 ± 0.1	11.9 ± 0.1	13.8 ± 0.1	10.4 ± 0.1	10.6 ± 0.1	11.5 ± 0.1	9.3 ± 0.2	9.8 ± 0.2	10.6 ± 0.1
χ^2	3.4	11	44	3.8	5.6	7.0	4.9	4.0	3.1	8.7	7.0	7.1
c (10^{-6} mol/mL)	4.45 ± 0.1	4.41 ± 0.1	4.36 ± 0.1	4.45 ± 0.1	4.41 ± 0.1	4.36 ± 0.1	4.46 ± 0.1	4.41 ± 0.1	4.37 ± 0.1	4.46 ± 0.1	4.41 ± 0.1	4.37 ± 0.1
N_{agg}	228	330	299	226	267	206	237	146	191	170	139	180
n (10^{16} cm^{-3})	1.18	0.81	0.88	1.19	0.99	1.27	1.13	1.82	1.38	1.58	1.91	1.46
ϕ_{tot}	0.09	0.09	0.09	0.09	0.10	0.14	0.08	0.14	0.13	0.09	0.12	0.14
ρ_{core} (10^{10} cm^{-2})	1.49	0.83	1.11	1.68	1.69	2.20	1.44	2.20	2.16	1.62	2.21	2.18
ρ_{shell} (10^{10} cm^{-2})	5.03	4.88	4.83	5.02	5.00	5.04	5.02	5.20	5.17	4.99	5.07	5.13
x (%)	90	87	86	90	90	90	89	93	92	89	91	92
y_{PO} (%)	48	46	41	46	34	25	50	32	26	48	32	26
y_{EO} (%)	3	0	0	4	3	0	5	2	3	5	2	2
y_{water} (%)	20	6	12	23	23	32	17	31	29	21	31	30
y_{SA} (%)	29	48	47	27	40	43	28	35	42	26	35	42
R_{SA} model	17.8	31.8	34.1	17.8	35.5	53.4	20.7	41.5	62.2	20.7	41.5	62.2
R_{SA}	17.8	35.5	53.4	17.8	35.5	53.4	20.7	41.5	62.2	20.7	41.5	62.2

[a] Results are given for TMB and toluene at 20 and 40°C for three increasing concentrations, C1, C2, and C3 (see Table 1). Notations are given in the theoretical model section. The solvent SLD ρ_0 equals 5.54 × 10^{10} cm^{-2} at 20°C and 5.50 × 10^{10} cm^{-2} at 40°C.

11324

dx.doi.org/10.1021/jp200212g |*J. Phys. Chem. B* 2011, 115, 11318–11329

Figure 2. (a) Effect of the temperature: SANS scattering curves obtained at 20, 40, and 60 °C for P123 in 1.6 M HCl. (b) Comparison of SANS and SAXS results in absolute scale (cm^{-1}) for P123 solutions in 1.6 M HCl at 40 °C: SANS with D_2O as the solvent (a), SAXS with H_2O as the solvent recorded at ESRF (b), and at the SOLEIL synchrotron (c). Symbols are used for the experimental data points and curves for the fit results (Tables 3 and 4).

sample	T_{onset} (°C)	ΔH (kJ.mol^{-1})
D_2O	16.0	425.8
HCl 2.5 M	22.0	316.9

Figure 3. Effect of HCl on the P123 micellization temperature. The DSC traces are obtained for two samples: 2.5 wt % P123 in D_2O (bottom curve) and 2.5 wt % P123 in 2.5 M HCl (upper curve). The values of T_{onset} and of the micellization enthalpy are given, where T_{onset} is defined as the temperature at the intersection of the tangent drawn through the first inflection point of the heat capacity peak with the baseline.

rationalize the optimum reaction conditions for the preparation of SBA-15. At 40 °C, spherically shaped Pluronic micelles are characterized by a very narrow size distribution having a well-defined almost dehydrated core and a hydrophilic corona. At temperatures below 15−20 °C, the micelles are not formed in the acidic solutions, whereas above 60 °C, a different phase is formed. The addition of HCl up to 2.5 M does not significantly change the structure of the micelles, with only a slight decrease of the core size. At the acid concentration over 6 M no micelles are detected, which is in agreement with the literature data indicating chemical instability of Pluronic P123 at very low pH (degradation of the PEO blocks).[28] It should be noted that from both the literature data and our results, no formation of SBA-15 materials is observed at HCl concentration above 4 M. Although well-defined micelles of Pluronic are present at low concentrations of acid, corresponding to pH > 2, the SBA-15 structure also is not formed owing to the very low rate of hydrolysis of the silica precursor such as TEOS.

Effect of the Nature of the Acidic Source (SAXS). The SAXS results for P123 solutions at 40 °C with different acids (HNO$_3$, HBr, HCl, H$_2$SO$_4$, and H$_3$PO$_4$) at the same concentration (Table SI) are given in Figure 4 and Table 4. A noticeable influence of the nature of the anion on the experimental curves is observed, as the positions of the form factor minima are strongly

shifted depending on the anions, with only H_2SO_4 and H_3PO_4 giving similar curves (Figure 4). Note that only q values greater than 2.0×10^{-2} Å^{-1} are taken into account in the fitting procedure, as the intensity measurements in the lower q range may be not entirely reliable because of the low signal intensity compared to the background ones. The overall size of the micelles is increasing, following the Hofmeister anions series:[28] (NO$_3^-$, Br$^-$, Cl$^-$, SO$_4^{2-}$, and H$_2$PO$_4^-$) (Table 4). The smallest size is obtained for the more salting-in/chaotropic anion NO$_3^-$ (R_{core} = 4.5 nm and R_{tot} = 6.5 nm), as the largest ones is obtained for the more salting-out/kosmotropic anion H$_3$PO$_4^-$ (R_{core} = 5.8 nm and R_{tot} = 9.6 nm). Making the assumption for SAXS that the core region contains only the PPO groups, increasing aggregation numbers are found accordingly, with N_{agg} = 57 ± 3 for HNO$_3$ and N_{agg} = 122 ± 6 for H$_3$PO$_4$.

The contrast parameter α is always negative for SAXS and it has a large variation depending on the acid (between −1.4 and −0.2). To interpret these variations, one has first to take into account the fact that, because the acidic solutions are concentrated, the bulk electron densities are significantly different from one acid to another and it is always greater than for pure water. The bulk electron density ρ_0 of the different acidic solutions (Table 4) have been calculated using literature data at 40 °C.[23] Moreover, because the counterions concentration in the shell region may be different to that of the bulk, the possibility to have a different value for the solvent electron density $\rho_{shell\ sol}$ in the shell region is assumed in the model (see SI section for details). For the more salting-out/kosmotropic anions (HCl, H_2SO_4, and H_3PO_4 as acidic sources), the values of $\rho_{shell\ sol}$ and ρ_0 are very close, indicating that these anions have no tendency to confine specifically within the micelles. In the case of HNO$_3$ and HBr, $\rho_{shell\ sol}$ is significantly greater than ρ_0, indicating that the salting-in/chaotropic anions NO$_3^-$ and Br$^-$ have a tendency to confine inside the micelles, as it is expected for these type of anions.[29]
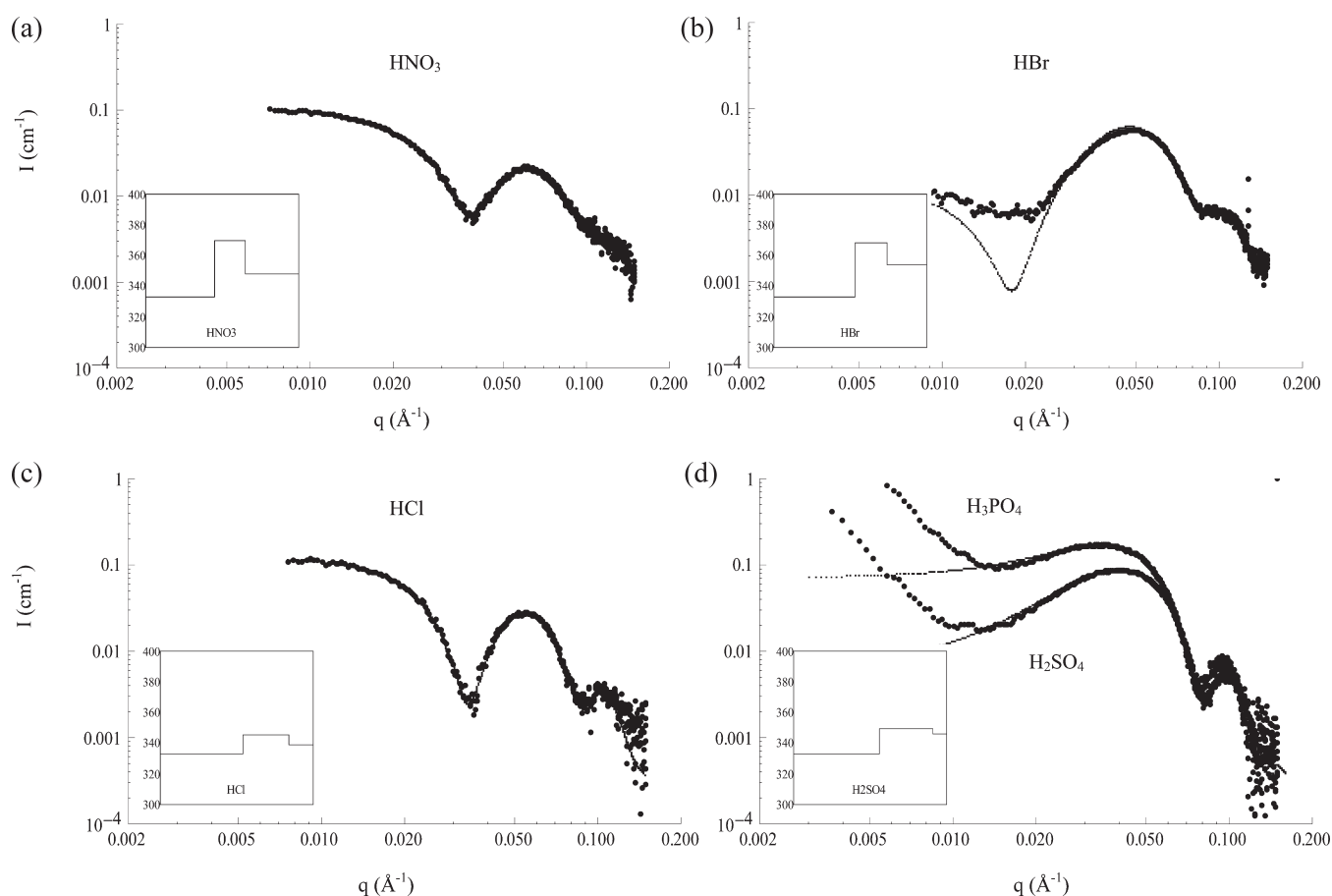
Figure 4. Effect of the nature of the acid source. SAXS results (SOLEIL synchrotron) in 1.6 M HCl at 40 °C with different acids: (a) HNO_3 (b) HBr, (c) HCl (d) H_2SO_4, and H_3PO_4. The corresponding electron density profiles are given in the insets in e/nm^3 units using the same radii range 0−10 nm. Detailed compositions are given in Table SI and fit results in Table 4.
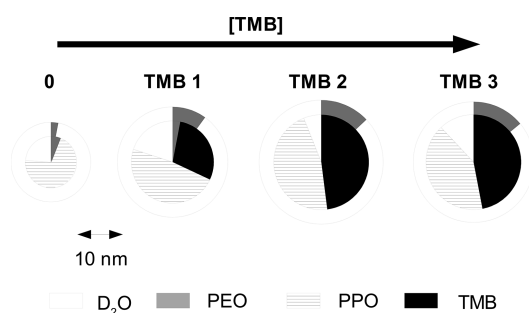
Figure 5. Effect of the addition of TMB on the P123 micelle size and composition in 1.6 M HCl at 20 °C. Values are given in Table 5.

For all the different acids, the estimated hydration level of the shell are similar, with solvent volume fractions x ranging from 80 to 90%. In Figure 4, the obtained electron density profiles in e/nm^{-3} are given in the insets (see more details in the S.I. section about the derivation of the electron density levels). From these profiles, one can see that the contrast between the shell region and the solvent is less and less pronounced following the Hofmeister anions series.

Effect of the Addition of Swelling Agent (SANS). The effect of different swelling agents on the structure of P123 micelles has been investigated at 20 and 40 °C using two different compounds: toluene (C_7H_8: TOL) and trimethylbenzene (C_9H_{12}: TMB) (Table 5). Samples with increasing concentrations (C1, C2, and C3) of the swelling agent have been prepared (Table 1) using 1.6 M aqueous solution of HCl. A considerable effect of the swelling agents on the structure of P123 micelles upon the addition of both toluene and TMB has been observed. The micelle dimensions (R_{core} and R_{tot}) and the polydispersity increase with the concentration of the swelling agent (Table 5). Compared to the sample in the same solvent, 1.6 M HCl, containing no swelling agent (Table 3), the overall size of P123 micelle increases from ~18 to ~25 nm, depending on the quantity of swelling agent added. Interestingly, no strong influence of the temperature between 20 and 40 °C (Table 5) is observed for any of the samples. Lastly, the polydispersity increases by a few percents with the concentration of the swelling agent for all samples (Table 5).

For TMB, the size of micelles increases significantly for TMB C1 and TMB C2 samples as compared to the P123 sample in 1.6 M HCl; however, a further increase in TMB concentration does not lead to micellar growth, micelles in TMB C3 sample have almost the same size as those in TMB C2. This indicates that the maximum swelling of the micelles by adding TMB is reached. In the case of toluene, the size of the micelles is still significantly increasing from concentration C2 to C3, indicating that larger quantities of toluene may be incorporated within the micelles.

From the absolute scaling (value of A in cm^{-7}) obtained from the fit, it is possible to determine the volume fraction of each
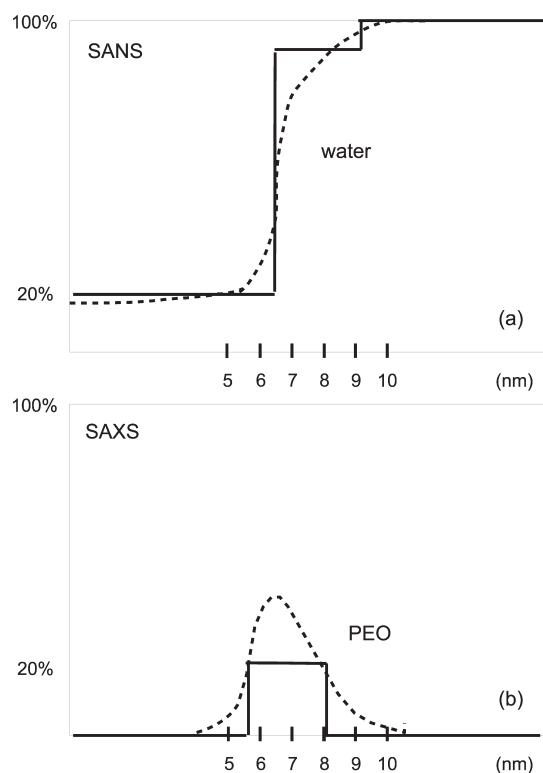
Figure 6. Radial distributions inside the micelles of water (a) and of PEO (b) (volume fractions) as derived from the core−shell model (solid lines). The distributions are obtained from the experiments at 40 °C in 1.6 M HCl, using SANS for water and SAXS for PEO. More realistic smooth distributions are depicted using dashed curves.

species in the shell and core region (Table 5 and Figure 5) assuming a model for the repartition of the different components inside the micelles (see the SI for more details). As for micelles containing no swelling agent, the shell region is assumed to contain only EO groups and the solvent, which allows the determination of the hydration level inside the shell. The core is assumed to contain the remaining EO groups if any, all the PO groups, toluene or TMB, and D_2O. The proportions of these four components in the core are determined assuming that both all the P123 copolymers and all the added swelling agent are inside the core of the micelles.

A macroscopic phase separation of the swelling agent may have occurred for the more concentrated samples, as seen by visual observation of the samples. To take this effect into account, we assumed in the case of TMB (at 20 °C, concentrations C2 and C3) that no EO groups are inside the core so that the proportion of the swelling agent inside the core is a free parameter. Then, we find that a maximum amount of TMB can be incorporated at 20 °C within the micelles corresponding to a TMB to P123 ratio R_{SA} of about 35 (Table 5 and Figure 5). As the temperature of the TMB-containing system is increased from 20 to 40 °C, all the TMB could be incorporated into the micelles.

In the case of TOL, it is always possible to derive an aggregation number and a composition of the micelles (Table 5) that are compatible with the hypothesis that all of the P123 copolymers and all TOL are incorporated within the micelles. But again, as a macroscopic phase separation of TOL may have happened in the more concentrated samples, the amount of incorporated TOL within the micelles derived from the model may be overestimated.

■ DISCUSSION

There are only very few combined SANS and SAXS studies of "Pluronic" triblock-copolymers in the micellar state (Pluronic P85 $(EO_{25}PO_{40}EO_{25})$,[11,18] and several studies using either SANS only[29] or SAXS only (Pluronic P123).[17] By combining both SANS and SAXS data, in the framework of a simple core−shell model, reliable values of the concentration and aggregation numbers of the micelles can be obtained. For the systems containing D2O as a solvent, SANS provide a very good contrast, and the core−shell model allows one to determine the distribution of the solvent inside the micelle with a high degree of precision. Since the contrast is very weak for SAXS, it is more difficult to derive a comparable quantitative description as in the case of SANS. The choice of the values used for the electron density levels (Tables 2 and 4) for the interpretation of the SAXS results is crucial because of the low contrast. For SAXS, the contrast is essentially a "shell" type one,[15] and in pure water at 20 and 40 °C, only EO chains contribute to the shell contrast, because the electron density of PO is very close to that of water (Table 2). In Figure 6, the structure of the micelles at 40 °C in 1.6 M HCl, is illustrated. The distributions of water and EO groups within the P123 micelles according to the core−shell model are drawn in solid lines. The main limitation of the core−shell model is the imposed constant densities inside the core and shell region; more realistic smooth distributions of water and EO are also shown in dashed lines. From Figure 6, useful information about the distribution of the PO and EO chains can be derived. The PO chains are located inside a 5.6 nm radius spherical region. The hydrophobic core (determined by SANS) has a radius of 6.3 nm and its hydration is about 20% vol. Fraction. The overall hydration level of the EO chain is high (80−90% vol fraction of water), but there is a gradient of hydration of the EO groups. The EO groups are probably less hydrated in the region located between 5.6 and 6.3 nm. The smooth distributions are drawn in order to illustrate this gradient of hydration, as it is not included in the core/shell model. Interestingly, the repartition of the PO and EO groups we obtain for the P123 micelles is in good agreement with the results for a similar triblock copolymer $(EO_{25}PO_{40}EO_{25})$ by modeling SANS data using a model based on Monte Carlo simulations.[19]

In acidic solutions, the counterion concentration in the shell may be different to that of the bulk, and this is taken into account in the model for SAXS. At the acidic pH, EO groups are protonated which induce a gradient of the counterion concentration within the shell. Indeed, this effect plays an important role in the reaction mechanism $(S° H^+)(X^- I^+)$ of the SBA-15 synthesis.[1,9,29,31] Even if it is not possible to quantify precisely the confinement of the anions in the shell in the framework of the simple model adopted here, our results show that the salting-in/chaotropic anions NO_3^- and Br^- have a tendency to confine inside the micelles, as it is expected for these type of anions.[29] The addition of HCl does affect the position of the micellization peak in DSC which is shifting toward higher temperatures. At the same time, the structure of the micelles does not change much with the HCl concentration at 40 °C as only a slight decrease of the core size is observed and micellization of the P123 molecules is almost complete at this temperature. This is in contrast with ref 28 where a much stronger influence of the addition of HCl on the micellar state has been proposed, although for a higher HCl concentration (3 M rather than 2.5 M). The addition of HCl (up to 2.5 M concentration) does not significantly change the

structure of the micelles, with only a slight decrease of the core size.

In the presence of toluene and TMB, the behavior of micelles is noticeably different demonstrating a significant increase in the micelle size, attributed to the swelling of the core of the micelles by the incorporation of the swelling agent. Saturation of the micellar growth beyond a certain concentration of the hydrophobic molecule is observed, which is related to the macroscopic phase separation detected for the more concentrated samples. For TMB, the results are in agreement with a previous SANS investigation.[30] The maximum relative amount of TMB that could be incorporated at 20 °C within the micelles is determined as $R_{SA} = 35$.

■ CONCLUSION

By combining both SANS and SAXS data, a detailed quantitative description of the micelles of P123 has been successfully obtained using a simple core—shell spherical model. The size, concentration and scattering contrast of the micelles have been measured in absolute scale both for SANS and SAXS. Making use of the known densities, the aggregation number of the micelles and their detailed composition are determined.

Our results show that the P123 micelles are always spherical before the addition of the inorganic precursor. In pure water, 40 °C is the optimum temperature to obtain well formed micelles. The addition of HCl up to 2.5 M concentration has very little effect on the structure of the micelles (the presence of HCl is of course essential for the synthesis of SBA materials following the addition of the inorganic precursor such as TEOS). However, a chemical degradation of the copolymer in stronger acidic conditions has been observed. The increase in size of the micelles upon the addition of the swelling agents (toluene and TMB) has been quantified in details. Finally, the structure of the micelles is influenced by the nature of the anions coming from the acidic source. Following the Hoffmeister serie, the micelles are smaller and more polydisperse with salting-in anions than with salting-out anions.

An important consequence of the fact that the P123 micelles are found to be always spherical is that the transition from spherical to cylindrical micelles observed during the SBA-15 synthesis[2−5] is most probably driven by the presence of inorganic species around the micelles. The formation of these mixed organic—inorganic cylindrical micelles has been recently confirmed by an in situ SAXS study of the SBA-15 synthesis performed at room temperature and pH close to 3.[32,33]

In a following paper,[9] we utilize the core—shell model to establish the structure of the hybrid organic—inorganic micellar species formed in the reaction mixture, focusing on the influence of the synthesis conditions on the formation mechanism of composite organic—inorganic materials after the addition of an inorganic precursor, and relating the structure of the final material to that of the micelles in the initial state.

■ ASSOCIATED CONTENT

ⓢ Supporting Information. Further details of the modeling procedures and additional figure SI and Table SI. This material is available free of charge via the Internet at http://pubs.acs.org.

■ AUTHOR INFORMATION

Corresponding Author
*Tel.: + 33 1 69 15 60 59. Fax: +33 1 69 15 60 86. E-mail: marianne.imperor@u-psud.fr.

Present Addresses
○Instituto de Física, Universidade de São Paulo, Caixa Postal 66318, 05314—970 São Paulo, Brasil.

■ REFERENCES

(1) Zhao, D. Y.; Huo, Q. S.; Feng, J. L.; Chmelka, B. F.; Stucky, G. D. Nonionic triblock and star diblock copolymer and oligomeric surfactant syntheses of highly ordered, hydrothermally stable, mesoporous silica structures. *J. Am. Chem. Soc.* **1998**, *120* (24), 6024–6036.

(2) Khodakov, A. Y.; Zholobenko, V. L.; Imperor-Clerc, M.; Durand, D. Characterization of the initial stages of SBA-15 synthesis by in situ time-resolved small-angle X-ray scattering. *J. Phys. Chem. B* **2005**, *109* (48), 22780–22790.

(3) Imperor-Clerc, M.; Grillo, I.; Khodakov, A. Y.; Zholobenko, V. L.; Durand, D. New insights into the initial steps of the formation of SBA-15 materials: an in situ small angle neutron scattering investigation. *Chem. Commun.* **2007**, *8*, 834–836.

(4) Ruthstein, S.; Schmidt, J.; Kesselman, E.; Talmon, Y.; Goldfarb, D. Resolving intermediate solution structures during the formation of mesoporous SBA-15. *J. Am. Chem. Soc.* **2006**, *128* (10), 3366–3374.

(5) Zholobenko, V. L.; Khodakov, A. Y.; Imperor-Clerc, M.; Durand, D.; Grillo, I. Initial stages of SBA-15 synthesis: An overview. *Adv. Colloid Interface Sci.* **2008**, *142* (1−2), 67–74.

(6) Ganguly, R.; Aswal, V. K.; Hassan, P. A.; Gopalakrishnan, I. K.; Yakhmi, J. V. Sodium chloride and ethanol induced sphere to rod transition of triblock copolymer micelles. *J. Phys. Chem. B* **2005**, *109* (12), 5653–5658.

(7) Aswal, V. K.; Wagh, A. G.; Kammel, M. Formation of rodlike block copolymer micelles in aqueous salt solutions. *J. Phys.: Condens. Matter* **2007**, *19*, 11.

(8) Denkova, A. G.; Mendes, E.; Coppens, M. O. Effects of salts and ethanol on the population and morphology of triblock copolymer micelles in solution. *J. Phys. Chem. B* **2008**, *112* (3), 793–801.

(9) Manet, S.; Schmitt, J.; Imperor-Clerc, M.; Zholobenko, V. L.; Durand, D.; Oliveira, C. L. P.; Pedersen, J. S.; Gervais, C.; Baccile, N.; Babonneau, F.; Grillo, I.; Meneau, F.; Rochas, C. Kinetics of the formation of 2D-hexagonal silica nano-structured materials by non-ionic block copolymer templating in solution *J. Phys. Chem. B* **2011**, *115*, 10.1021/jp200213k.

(10) Mortensen, K.; Pedersen, J. S. Structural Study on the Micelle Formation of Poly(Ethylene Oxide) Poly(Propylene Oxide) Poly-(Ethylene Oxide) Triblock Copolymer in Aqueous-Solution. *Macromolecules* **1993**, *26* (4), 805–812.

(11) Glatter, O.; Scherf, G.; Schillen, K.; Brown, W. Characterization of A Poly(Ethylene Oxide) Poly(Propylene Oxide) Triblock Copolymer (Eo(27)-Po39-Eo(27)) in Aqueous-Solution. *Macromolecules* **1994**, *27* (21), 6046–6054.

(12) Jain, N. J.; Aswal, V. K.; Goyal, P. S.; Bahadur, P. Micellar structure of an ethylene oxide propylene oxide block copolymer: A small-angle neutron scattering study. *J. Phys. Chem. B* **1998**, *102* (43), 8452–8458.

(13) Liu, Y. C.; Chen, S. H.; Huang, J. S. Small-angle neutron scattering analysis of the structure and interaction of triblock copolymer micelles in aqueous solution. *Macromolecules* **1998**, *31* (7), 2236–2244.

(14) Goldmints, I.; Yu, G. E.; Booth, C.; Smith, K. A.; Hatton, T. A. Structure of (deuterated PEO) (PPO) (deuterated PEO) block copolymer micelles as determined by small angle neutron scattering. *Langmuir* **1999**, *15* (5), 1651–1656.

(15) Jansson, J.; Schillen, K.; Nilsson, M.; Soderman, O.; Fritz, G.; Bergmann, A.; Glatter, O. Small-angle X-ray scattering, light scattering,

11328

dx.doi.org/10.1021/jp200212g |*J. Phys. Chem. B* 2011, 115, 11318–11329

and NMR study of PEO-PPO-PEO triblock copolymer/cationic surfactant complexes in aqueous solution. *J. Phys. Chem. B* **2005**, *109* (15), 7073–7083.

(16) Lof, D.; Niemiec, A.; Schillen, K.; Loh, W.; Olofsson, G. A calorimetry and light scattering study of the formation and shape transition of mixed micelles of EO20PO68EO20 triblock copolymer (P123) and nonionic surfactant (C12EO6). *J. Phys. Chem. B* **2007**, *111* (21), 5911–5920.

(17) Soni, S. S.; Brotons, G.; Bellour, M.; Narayanan, T.; Gibaud, A. Quantitative SAXS analysis of the P123/water/ethanol ternary phase diagram. *J. Phys. Chem. B* **2006**, *110* (31), 15157–15165.

(18) Pedersen, J. S. Analysis of small-angle scattering data from colloids and polymer solutions: modeling and least-squares fitting. *Adv. Colloid Interface Sci.* **1997**, *70*, 171–210.

(19) Pedersen, J. S.; Gerstenberg, M. C. The structure of P85 Pluronic block copolymer micelles determined by small-angle neutron scattering. *Colloids Surf. A-Physicochem. Eng. Aspects* **2003**, *213* (2−3), 175–187.

(20) Willner, L.; Poppe, A.; Allgaieri, J.; Monkenbusch, M.; Lindner, P.; Richter, D. Micellization of amphiphilic diblock copolymers: Corona shape and mean-field to scaling crossover. *Europhys. Lett.* **2000**, *51* (6), 628–634.

(21) Glatter, O. http://physchem.kfunigraz.ac.at/sm/ *Scattering methods home page*, Karl-Franzens University, Graz, Austria, 2009.

(22) NIST database. http://www.ncnr.nist.gov/resources/n-lengths/. NIST 2009.

(23) Novotny, P.; Söhnel, O. Densities of Binary Aqueous Solutions of 306 Inorganic substances. *J. Chem. Eng. Data* **1988**, *33*, 49–55.

(24) Sommer, C.; Pedersen, J. S.; Stein, P. C. Apparent specific volume measurements of poly(ethylene oxide), poly(butylene oxide), poly(propylene oxide), and octadecyl chains in the micellar state as a function of temperature. *J. Phys. Chem. B* **2004**, *108* (20), 6242–6249.

(25) Pedersen, J. S., Resolution Effects and Analysis of Small-angle Neutron Scattering Data. *J. Phys. IV France* **1994**, Coll. *C8 3*, 491-498; Grillo, I. Small-Angle Neutron Scattering and Applications in Soft Condensed Matter. In *Soft-matter Characterization*; Borsali, R., Pecora, R., Eds.; Springer: New York, 2008; Chapter 13, Vol. XXXVI.

(26) Wanka, G.; Hoffmann, H.; Ulbricht, W. Phase diagrams and aggregation behavior of poly(oxyethylene)-poly(oxypropylene)-poly-(oxyethylene) triblock copolymers in aqueous solutions. *Macromolecules* **1994**, *27*, 4145–4159.

(27) Olofsson, G.; Wang, G. Polymer Surfactant Systems. In *Surfactant Science Series*; Kwak, J. C. T., Ed.; Marcel Dekker: New York, 1998; pp 193−238.

(28) Yang, B.; Guo, C.; Chen, S.; Ma, J. H.; Wang, J.; Liang, X. F.; Zheng, L.; Liu, H. Z. Effect of acid on the aggregation of poly(ethylene oxide)-poly(propylene oxide)-poly(ethylene oxide) block copolymers. *J. Phys. Chem. B* **2006**, *110* (46), 23068–23074.

(29) Leontidis, E. Hofmeister anion effects on surfactant self-assembly and the formation of mesoporous solids. *Curr. Opin. Colloid Interface Sci.* **2002**, *7* (1−2), 81–91.

(30) Lettow, J. S.; Lancaster, T. M.; Glinka, C. J.; Ying, J. Y. Small-angle neutron scattering and theoretical investigation of poly(ethylene oxide)-poly(propylene oxide)-poly(ethylene oxide) stabilized oil-in-water microemulsions. *Langmuir* **2005**, *21* (13), 5738–5746.

(31) Newalkar, B. L.; Komarneni, S. Control over microporosity of ordered microporous-mesoporous silica SBA-15 framework under microwave-hydrothermal conditions: Effect of salt addition. *Chem. Mater.* **2001**, *13* (12), 4573–4579.

(32) Sundblom, A.; Oliveira, C. L. P.; Palmqvist, A. E. C.; Pedersen, J. S. Modeling in Situ Small-Angle X-ray Scattering Measurements Following the Formation of Mesostructured Silica. *J. Phys. Chem. C* **2009**, *113* (18), 7706–7713.

(33) Sundblom, A.; Oliveira, C. L. P.; Pedersen, J. S.; Palmqvist, A. E. C. On the Formation Mechanism of Pluronic-Templated Mesostructured Silica. *J. Phys. Chem. C* **2010**, *114*, 3483–3492.